

Communication

## Observation of Long-Range Vicinal Effect in Chiral Cu(II)-Cr(VI) or Cu(II)-W(VI) Bimetallic Coordination Polymers

Naoshi Hayashi and Takashiro Akitsu \*

Department of Chemistry, Faculty of Science, Tokyo University of Science, 1-3 Kagurazaka, Shinjuku-ku, Tokyo 162-8601, Japan

\* Author to whom correspondence should be addressed; E-Mail: akitsu@rs.kagu.tus.ac.jp; Tel.: +81-3-5228-8271; Fax: +81-3-5261-4631.

Received: 13 May 2011; in revised form: 17 June 2011 / Accepted: 28 June 2011 /

Published: 29 June 2011

---

**Abstract:** We have prepared some diastereomers of  $[\text{CuL}_2][\text{M}_2\text{O}_7]$  (L is 1,2-diaminocyclohexane and its derivatives; M = Cr and W) bimetallic coordination polymers and confirmed their structural similarity and inner electronic states by means of XRD and XAS, respectively. For the first time, we have successfully observed distant vicinal effect of which the chiral source is only chiral organic ligands of  $[\text{CuL}_2]^{2+}$  moieties (acting as ligand complex), while probe bands for solid state CD spectra are charge transfer (CT) bands of  $[\text{M}_2\text{O}_7]^{2-}$  moieties (achiral complex) with the  $d^0$  electronic configuration. The new concept (interpretation) of this observation will be important for supramolecular chirality of coordination polymers built by ligand complexes.

**Keywords:** chirality; copper; CD; XRD; XAS

---

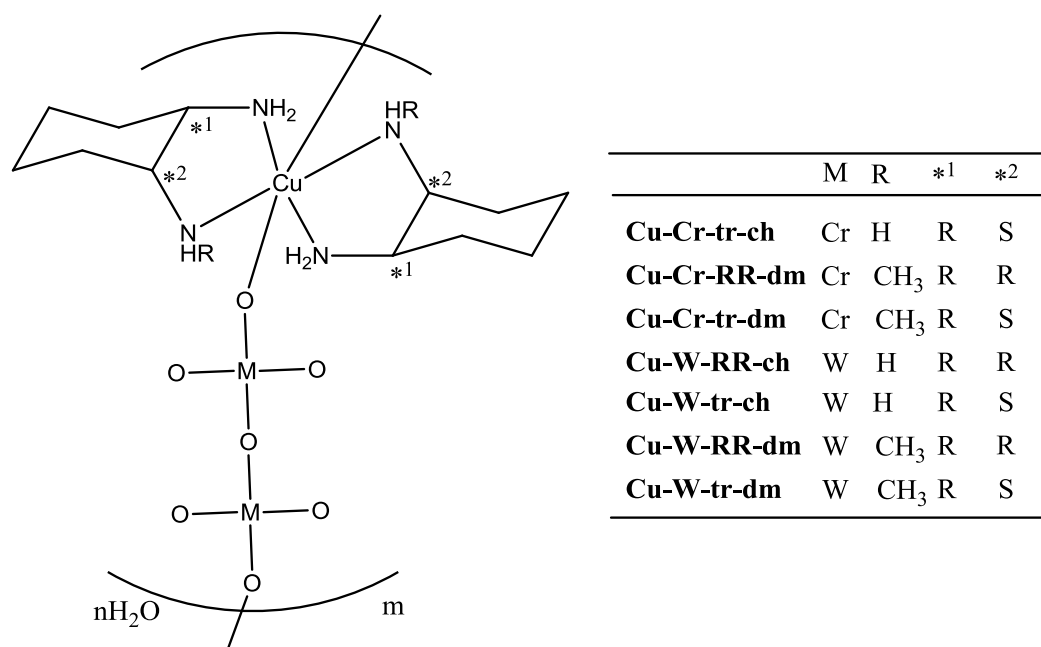
### 1. Introduction

Recently we have proposed a new concept of “supramolecular vicinal effect”, which is long-range induced chiroptical observation of an achiral unit from non-bonded (supramolecular assemblies) or weakly surrounded (host-guest co-crystal) chiral sources [1]. It is different to the normal vicinal effect (observation of CD bands in d-d region from chiral ligands through coordination bonds) [2,3] or

conventionally induced CD of many supramolecular assemblies [4,5]. As for chiral coordination polymers, thermally-accessible lattice strain and local pseudo Jahn-Teller distortion of  $[\text{CuL}_2]_3[\text{M}(\text{CN})_6]_2 \cdot 4\text{H}_2\text{O}$  ( $\text{L} = \text{trans-cyclohexane-}(1R, 2R)\text{-diamine}$ ;  $\text{M} = \text{Cr, Co, and Fe}$ ) [6] have been reported. In its crystal packing of co-crystals of one-dimensional cyanide-bridged  $\text{Cu(II)-Cr(III)}$ , and  $\text{Cu(II)-Co(III)}$  bimetallic assemblies and mononuclear  $\text{Cu(II)}$  complexes, (pseudo) Jahn-Teller effect play an important role in flexible distortion of crystal structures especially in the  $\text{Cu(II)}$  coordination environment. Moreover, we prepared their H/D isotope derivatives to confirm Jahn-Teller effect [7]. Though solid-state CD spectra were also measured, supramolecular co-crystals of chiral components makes their chiroptical properties difficult to understand.

Herein, we have prepared some diastereomers of  $[\text{CuL}_2][\text{M}_2\text{O}_7]$  ( $\text{L}$  is 1,2-diaminocyclohexane and its derivatives;  $\text{M} = \text{Cr and W}$ ) bimetallic coordination polymers (Figure 1). For the solid state CD bands, charge transfer of  $[\text{M}_2\text{O}_7]^{2-}$  moieties result from long-range vicinal effect by chiral organic ligands of  $[\text{CuL}_2]^{2+}$  moieties (acting as ligand complex). In addition, there are only a few examples,  $[\text{Cu}(\text{ligands})][\text{Cr}_2\text{O}_7]$  [8], structurally characterized.

**Figure 1.** Molecular structures of the coordination polymers with abbreviations.



## 2. Results and Discussion

### 2.1. Solid State CD and Electronic Spectra

Figures 2, 3, and 4 show solid state CD (as KBr pellets) and diffuse reflectance electronic spectra for **Cu-Cr-RR-dm**, **Cu-W-RR-ch**, and **Cu-W-RR-ch**, respectively. The CD spectrum of **Cu-Cr-RR-dm** shows a negative peak at  $18,000\text{ cm}^{-1}$ , a negative peak at  $30,000\text{ cm}^{-1}$ , and a positive peak at  $37,000\text{ cm}^{-1}$ . The corresponding peaks in diffuse reflectance electronic spectra are  $20,000\text{ cm}^{-1}$ , and a rather broad band in the  $3,000\text{--}4,400\text{ cm}^{-1}$  region. While the diffuse reflectance electronic spectra (not shown) exhibit peaks or shoulders at  $17,000$ ,  $21,000$ ,  $26,000$ ,  $27,000$ , and  $38,000\text{ cm}^{-1}$  for **Cu-Cr-tr-ch** and  $17,000$ ,  $21,000$ ,  $25,000$ ,  $33,000$ , and  $38,000\text{ cm}^{-1}$  for **Cu-Cr-tr-dm**.

On the other hand, the CD spectrum of **Cu-W-RR-ch** shows a negative peak at  $18,000\text{ cm}^{-1}$ , which is the sole obvious peak. The corresponding peaks in diffuse reflectance electronic spectra are  $18,000$  and  $37,000\text{ cm}^{-1}$ . The CD spectrum of **Cu-W-RR-dm** shows a negative peak at  $17,000\text{ cm}^{-1}$  and a positive peak at  $34,000\text{ cm}^{-1}$ . The corresponding peaks in diffuse reflectance electronic spectra are  $17,000$ ,  $31,000$ , and  $38,000\text{ cm}^{-1}$ . While the diffuse reflectance electronic spectra (not shown) exhibit peaks or shoulders at  $18,000$  and  $37,000\text{ cm}^{-1}$  for **Cu-W-tr-ch** and  $17,000$ ,  $31,000$ , and  $38,000\text{ cm}^{-1}$  for **Cu-W-tr-dm**.

**Figure 2.** Solid state CD and diffuse reflectance electronic spectra for **Cu-Cr-RR-dm** (solid lines), the corresponding Cu-precursor (broken lines), and the Cr-precursor (dotted lines).

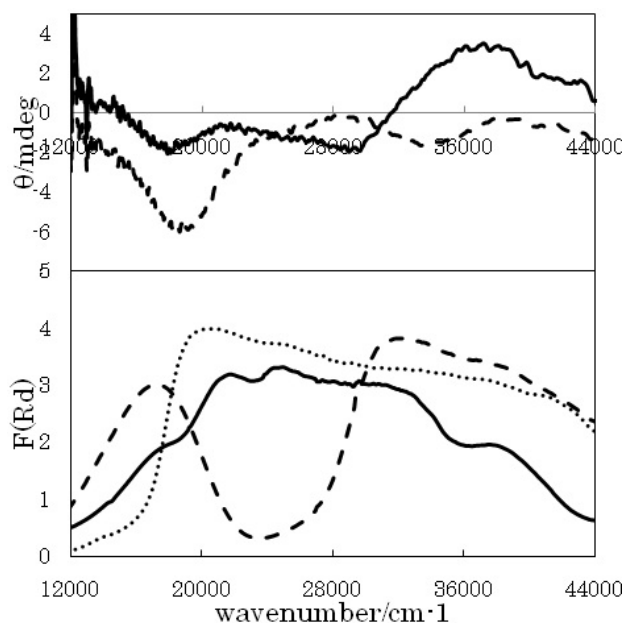


**Figure 3.** Solid state CD and diffuse reflectance electronic spectra for **Cu-W-RR-ch** (solid lines), the corresponding Cu-precursor (broken lines), and the W-precursor (dotted lines).

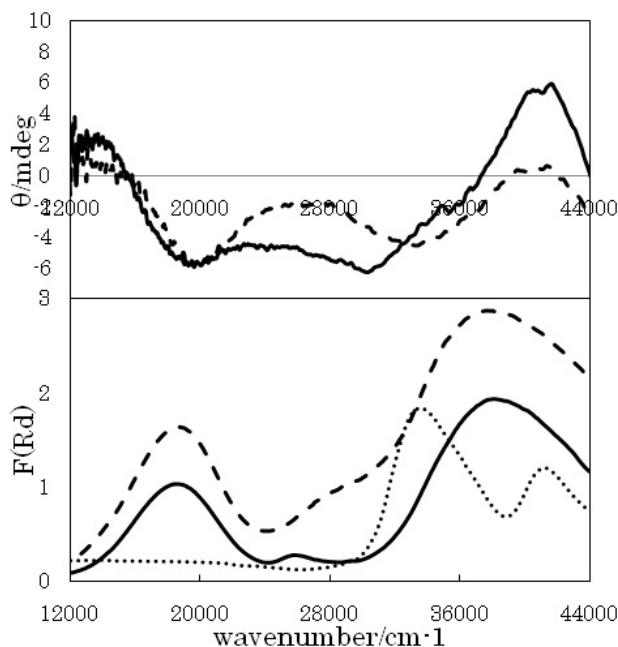
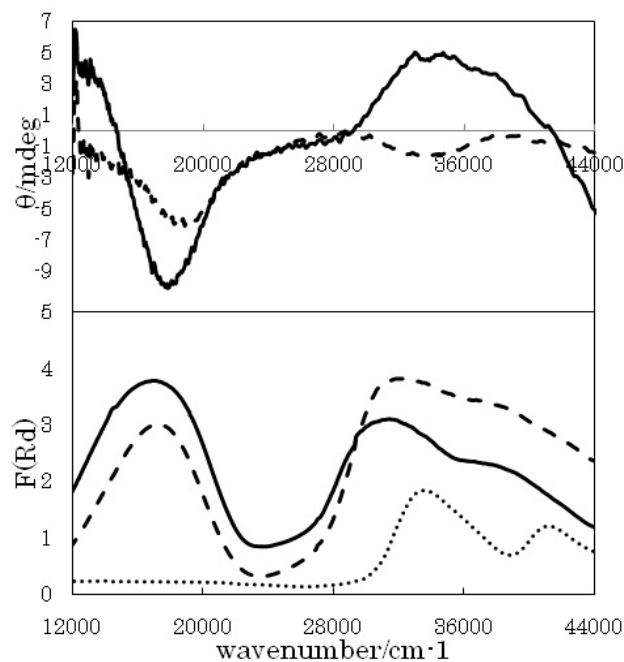


**Figure 4.** Solid state CD and diffuse reflectance electronic spectra for **Cu-W-RR-dm** (solid lines), the corresponding Cu-precursor (broken lines), and the W-precursor (dotted lines).



Systematic comparison of the related spectra and peaks of Cu-precursor at 17,000 (d-d) and 32,000 (CT)  $\text{cm}^{-1}$ , Cr-precursor at 20,000 (CT)  $\text{cm}^{-1}$ , and W-precursor at 32,000 and 40,000 (CT)  $\text{cm}^{-1}$  should be helpful for establishing assignment experimentally. It should be noted that CD bands in d-d region of Cu-precursor are attributed to vicinal effect by chiral organic ligand, while CD bands in CT region of CT band of bimetallic coordination polymers are attributed to vicinal effect by chiral complex ligand (namely the Cu-precursor). For example, a negative peak around 30,000  $\text{cm}^{-1}$  for **Cu-Cr-RR-dm** (Figure 2) is a typical CD band of long-range vicinal effect classified as a novel case.

## 2.2. Powder XRD Patterns

As mentioned above, the corresponding metal-substituted coordination polymers with identical ligands, indicate similar XRD patterns at room temperature except for the effect of metal ion size. Selected predominant peaks are also described in the experimental section. In the course work, we have investigated negative or positive thermal expansion of lattice and local bond compression or elongation about Jahn-Teller distortion of axial bonds, which are usually flexible. The aim of temperature dependence XRD measurement is to check there are no abnormal structural changes with changing temperatures.

For example, we measured powder XRD patterns (not shown) for **Cu-W-RR-ch** measured at 110–300 K with an interval of 10 K. The predominant peaks appeared at  $2\theta = 7.685, 12.905, 14.964, 16.936, 21.286, 24.853, 27.202, 27.840, 28.362, 29.377, 30.189, 31.117, 32.770, 33.959, 41.789, 43.500, \text{ and } 44.950$  degree at 110 K. On heating up to 300 K, the corresponding peaks appeared at  $2\theta = 7.656, 12.847, 14.906, 16.878, 21.228, 24.737, 27.057, 27.724, 28.246, 29.232, 30.073, 31.001, 32.625, 33.814, 41.615, 43.326, \text{ and } 44.776$  degrees at 300 K, *i.e.*, diffraction peaks shift to low-angles. Thermal shift features with detailed values for the most intense peaks are listed in Table 1.

Therefore, the crystal lattice normally exhibits positive thermal expansion depending on the temperature.

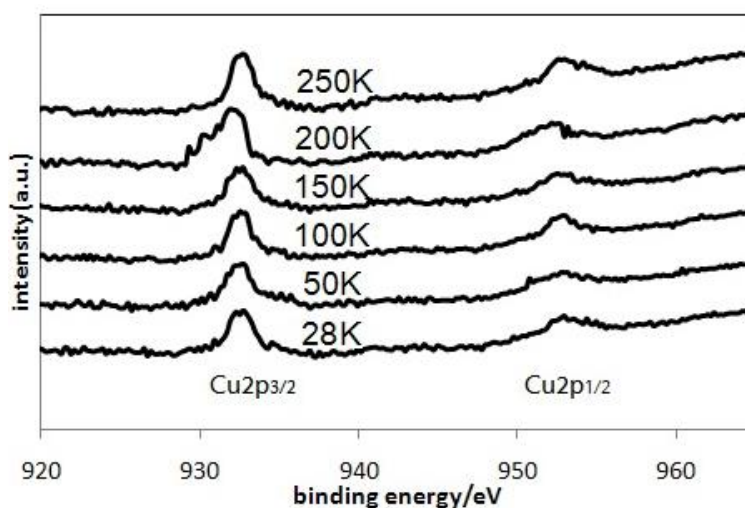
**Table 1.** Thermal shift features of the most intense peaks.

T/K	2 $\theta$ /degree	Intensity	Half width/degree
110	27.84	4,862	0.435
120	27.84	4,860	0.406
130	27.81	4,850	0.435
140	27.81	4,935	0.435
150	27.81	4,888	0.435
160	27.78	4,831	0.435
170	27.78	4,868	0.435
180	27.78	4,876	0.435
190	27.78	4,881	0.435
200	27.78	4,807	0.435
210	27.78	4,864	0.406
220	27.75	4,713	0.435
230	27.75	4,731	0.406
240	27.75	4,724	0.435
250	27.75	4,696	0.435
260	27.72	4,669	0.435
270	27.75	4,651	0.435
280	27.72	4,682	0.435
290	27.72	4,673	0.435
300	27.72	4,637	0.435

### 2.3. XAS Spectra

Figure 5 shows temperature dependence of soft X-ray absorption spectra (XAS) for **Cu-W-RR-ch** measured at 28, 50, 100, 150, 200, and 250 K. At each temperature, the Cu2p<sub>1/2</sub> and Cu2p<sub>3/2</sub> peaks appeared at about 952 and 932 eV, respectively. Absence of weak peaks between them suggests that valence state is not copper(I) nor mixed-valence of copper(I) and copper(II) but clearly copper(II). The bridging [Cr<sub>2</sub>O<sub>7</sub>]<sup>2-</sup> moieties did not contribute to delocalization of charges. In addition, little difference between temperature changes indicates that the electronic states of inner shells are stable.

**Figure 5.** Temperature dependence of XAS (Cu2p<sub>1/2</sub> and Cu2p<sub>3/2</sub> peaks) for **Cu-W-RR-ch**.



### 3. Experimental Section

**Materials.** All the reagents (Aldrich, TCI, and Wako) were commercially available and were used as received without further purification. The precursor mononuclear copper(II) complexes were prepared according to procedures in the literature (e.g., [4]) with corresponding starting compounds.

**Preparation of Cu-Cr-tr-ch.** Slow diffusion of an aqueous solution (45 mL) of the precursor (0.0150 g, 0.0423 mmol) onto an aqueous solution (5 mL) of Na<sub>2</sub>CrO<sub>4</sub> (0.0107 g, 0.0926 mmol) at 298 K gave rise to brown precipitates after several days. Yield 0.0032 g (14.0%). IR (KBr, cm<sup>-1</sup>): 938, 877 (Cr-O). XRD ( $\lambda = 1.54184 \text{ \AA}$ , 2 $\theta$ /degree): 7.946, 17.342, 19.082, 19.198, 20.909, 23.838, 29.638, 43.471.

**Preparation of Cu-Cr-RR-dm.** Yield 0.0041 g (17.6%). IR (KBr, cm<sup>-1</sup>): 936, 873 (Cr-O). XRD ( $\lambda = 1.54184 \text{ \AA}$ , 2 $\theta$ /degree): 9.135, 15.283, 17.835, 18.183, 19.865, 21.779, 23.954, 25.172, 27.202, 30.943.

**Preparation of Cu-Cr-tr-dm.** Yield 0.0048 g (20.0%). IR (KBr, cm<sup>-1</sup>): 935, 873 (Cr-O). XRD ( $\lambda = 1.54184 \text{ \AA}$ , 2 $\theta$ /degree): 6.989, 7.540, 8.207, 8.903, 10.324, 12.180, 12.992, 13.804, 14.500, 23.693, 28.449, 29.174.

**Preparation of Cu-W-RR-ch.** Yield 0.0251 g (70.2%). IR (KBr, cm<sup>-1</sup>): 852, 819 (W-O). XRD ( $\lambda = 1.54184 \text{ \AA}$ , 2 $\theta$ /degree): 16.878, 23.432, 27.724, 29.551, 32.654, 43.355.

**Preparation of Cu-W-tr-ch.** Yield 0.0218 g (61.0%). IR (KBr, cm<sup>-1</sup>): 852, 819 (W-O). XRD ( $\lambda = 1.54184 \text{ \AA}$ , 2 $\theta$ /degree): 7.279, 14.587, 16.878, 27.724, 29.522, 32.625, 39.208, 43.355.

**Preparation of Cu-W-RR-dm.** Yield 0.0141 g (40.0%). IR (KBr, cm<sup>-1</sup>): 852, 819 (W-O). XRD ( $\lambda = 1.54184 \text{ \AA}$ , 2 $\theta$ /degree): 16.878, 23.432, 27.724, 29.551, 32.654, 43.355.

**Preparation of Cu-W-tr-dm.** Yield 0.0113 g (32.0%). IR (KBr, cm<sup>-1</sup>): 852, 820 (W-O). XRD ( $\lambda = 1.54184 \text{ \AA}$ , 2 $\theta$ /degree): 12.847, 14.906, 16.820, 21.054, 21.199, 25.839, 27.057, 28.246, 29.232, 30.044, 31.001, 33.553, 33.814, 41.615, 44.747.

**Physical Measurements.** Infrared spectra were recorded as KBr pellets on a JASCO FT-IR 4200 plus spectrophotometer equipped with polarizer in the range of 4,000–400 cm<sup>-1</sup> at 298 K. Diffuse reflectance electronic spectra were measured on a JASCO V-570 UV/VIS/NIR spectrophotometer equipped with an integrating sphere in the range of 800–200 nm at 298 K. Circular dichroism (CD) spectra were measured as KBr pellets on a JASCO J-820 spectropolarimeter in the range of 800–200 nm at 298 K. Powder XRD patterns were also measured by using synchrotron radiation beamline at KEK-PF BL-8B (2010G511) with 8 keV ( $\lambda = 1.54184 \text{ \AA}$ ) with a RIGAKU imaging plate. The Cu2p<sub>3/2</sub> and Cu2p<sub>1/2</sub> peaks of XAS (soft X-ray absorption spectra) were measured at KEK PF BL-19B (2010G510) under variable temperature. The spectra were corrected by the standard Au sample.

### 4. Conclusions

In summary, we have prepared some diastereomers of [CuL<sub>2</sub>][M<sub>2</sub>O<sub>7</sub>] (L is 1,2-diaminocyclohexane and its derivatives; M = Cr and W) bimetallic coordination polymers and confirmed their structural similarity and inner electronic states for selected compounds. We have successfully observed distant vicinal effect in the chiral Cu(II)-Cr(VI) or Cu(II)-W(VI) bimetallic coordination polymers. The only chiral source is chiral organic ligands of [CuL<sub>2</sub>]<sup>2+</sup> moieties, while probe bands for solid state CD

spectra are charge transfer bands of  $[M_2O_7]^{2-}$  moieties with  $d^0$  electronic configuration. Furthermore a detailed study of an analogous complex (*Cu-Cr-RR-ch*), discussed as a single crystal, will be reported in a separate paper.

### Acknowledgments

This work with synchrotron radiation was carried out at KEK-PF BL-8B (2010G511) and BL-19B (2010G510).

### References

1. Akitsu, T. Syntheses, structure, and electronic properties of assemblies of diastereomers of nickel(II) complexes with tetracyanometalates  $[M(CN)_4]^{2-}$  (M = Ni, Pd, and Pt). In *Stereochemistry Research Trends*; Monika, M.A., Golob, J.H., Eds.; Nova Science Publishers, Inc.: New York, NY, USA, 2008; Chapter 4, pp. 107-128.
2. Mason, S.F. *Molecular Optical Activity & the Chiral Discriminations*; Cambridge University Press: Cambridge, UK, 1982.
3. Amouri, H.; Gruselle, M. *Chirality in Transition Metal Chemistry*; Wiley: Chichester, UK, 2008.
4. Koslowski, A.; Sreerama, N.; Woody, R.W. Theoretical approach to electronic optical activity. In *Circular Dichroism Principle and Applications*, 2nd ed.; Berova, N., Nakanishi, K., Woody, R.W., Eds.; Wiley-VCH: New York, NY, USA, 2000; pp. 55-96.
5. Akitsu, T.; Einaga, Y.; Yoza, K. Thermally-accessible lattice strain and local pseudo Jahn-Teller distortion in various dimensional  $Cu^{II}-M^{III}$  bimetallic cyanide-bridged assemblies. *Open Inorg. Chem. J.* **2008**, *1*, 1-10.
6. Akitsu, T.; Sonoki, S. Influence of water molecules on properties of binuclear or bridged structures for chiral  $Cu^{II}-Ni^{II}$ ,  $Cu^{II}-Pd^{II}$ , and  $Cu^{II}-Pt^{II}$  tetracyano-bimetallic assemblies. *Open Cryst. J.* **2011**, *4*, 8-15.
7. Jameson, G.B.; Seferiadis, N.; Oswald, H.R.  $\mu$ -Dichromato(VI)-O,O'-bis(ethylenediamine)copper(II): Structure, thermochemistry and magnetic susceptibility. *Acta Crystallographica* **1986**, *C42*, 984-987.

© 2011 by the authors; licensee MDPI, Basel, Switzerland. This article is an open access article distributed under the terms and conditions of the Creative Commons Attribution license (<http://creativecommons.org/licenses/by/3.0/>).